

Physical Properties of the Gas and Dust in the Orion B Molecular Cloud (L 1630)

Ralf Launhardt

*Astrophysical Institute and University Observatory, Schillergässchen
2-3, D-07745 Jena, Germany; launh@astro.uni-jena.de*

and

Elizabeth A. Lada

*Department of Astronomy, University of Florida, Gainesville, FL
32611-2055, USA*

Abstract.

In this chapter, the distribution of dense gas and dust in the Orion B (L 1630) Giant Molecular Cloud is discussed. Recent observational knowledge on the incidence, distribution, and properties of dense cores and protostellar condensations is reviewed. In particular, the relation between cloud clumps, dense cores, dust condensations, and star formation is analyzed. The discussion is mainly based on recent CS multi-transition studies and observations of the thermal mm dust continuum emission.

1. Introduction

Understanding the process of star formation is closely related to understanding the structure and evolution of the parental molecular clouds. Recent studies have shown that – contrary to low-mass stars, which also form in small molecular clouds (dark cloud complexes and globules) – high-mass stars form exclusively in Giant Molecular Clouds (GMCs, $M_{\text{cloud}} \gtrsim 10^5 M_{\odot}$) (see Shu et al. 1987, and Blitz 1993 for recent reviews of GMC properties).

There are currently two different general views of molecular cloud structure. One is that molecular clouds are fractal with no preferred length scale (e.g., Falgarone et al. 1991; Elmegreen & Falgarone 1996). The alternative view is that GMCs are built up of “clumps” on a preferred length scale of a few parsec which is determined by the forces of gravity, pressure, etc. (e.g., Blitz & Shu 1980). These clumps may be spheroidal, but are mostly filamentary. A clumpy structure can already be seen in low-resolution ^{12}CO maps. Using the rarer and more optically thin ^{13}CO isotope, smaller structures down to some tenth of a parsec can be resolved. It is not completely clear to what extent the observed clump properties are the result of observational selection, such as beam size or excitation conditions. There is, however, evidence that the clumps contain well-defined “dense cores” which can be mapped, e.g., in CS (e.g. Linke & Goldsmith 1980; Lada et al. 1991a, hereafter LBS; Tatematsu et al. 1993; Plume et al.

1997) or in NH_3 (e.g. Myers & Benson 1983; Benson & Myers 1989; Harju et al. 1991). Blitz & Williams (1997) showed for the Taurus Molecular Cloud that there is actually a change in the character of the cloud structure on a scale of 0.25–0.5 pc, close to the thermal Jeans length at the observed gas densities. To distinguish these units from the clumps described above, we call them dense “cores” (see Table 1).

These cloud cores are, however, not the progenitors of individual stars. Their masses are, in general, much higher than the masses of the stars they form and their mass spectrum (LBS; Tatematsu et al. 1993) differs significantly from that of the stellar initial mass function (IMF) (see discussion in Zinnecker 1990). What else are then the actual birthplaces of stars in a molecular cloud and how can one find them? Progress in this field has been made by using the millimetre dust continuum emission as a tracer which was only possible after the development of very sensitive broadband bolometer systems (see Mezger 1994 for a review). “Real” pre-protostellar and protostellar condensations with typical diameters of a few hundredths of a parsec, mean densities of $\geq 10^6 \text{ cm}^{-3}$, and masses which are not considerably higher than the masses of typical stars which are formed in the observed regions were identified during the past eight years by their thermal dust emission in isolated Bok globules (Chandler et al. 1990; Launhardt & Henning 1997), in dense cores of dark clouds (e.g. André et al. 1993; Ward-Thompson et al. 1994) as well as in dense cores in GMCs (e.g. Mezger et al. 1992).

Table 1. Global properties of GMCs and their substructures.

	Mass	Size	Volume Density	Column Density	Tracer
	M (M_\odot)	D (pc)	$n(\text{H}_2)$ (cm^{-3})	$N(\text{H}_2)$ (cm^{-2})	
GMC ^a	$\gtrsim 10^5$	~ 50	~ 50	$3 - 6 \times 10^{21}$	^{12}CO
Clump ^b	$10^3 - 10^4$	$2 - 5$	$10^2 - 10^3$	$10^{21} - 10^{22}$	^{12}CO , ^{13}CO
Dense core ^c	$10 - 500$	$0.1 - 0.5$	$\sim 10^4$	$10^{21} - 10^{22}$	^{13}CO , NH_3 , CS , H_2CO
Condensation ^d	$1 - 20$	$0.01 - 0.2$	$10^6 - 10^8$	$5 - 50 \times 10^{22}$	mm dust continuum, higher CS transitions

^aBlitz 1993; ^bShu et al. 1987, Goldsmith 1987; ^cLada et al. 1991a; ^dLaunhardt et al. 1996

Table 1 summarizes our current knowledge about the global properties of GMCs in the solar neighborhood and their observed substructures. Note that especially the definition of a clump is highly uncertain and that such clumps are observed over a wide range of sizes and masses. With the exception of so-called hot cores which are heated by newly formed high-mass stars (e.g. Genzel & Stutzki 1989), all these structures have gas temperatures of $T \sim 10 - 20 \text{ K}$.

Most stars in our galaxy form in GMCs. But, why do different GMCs have different star formation properties? Is this just an evolutionary effect or are there general morphological differences? What causes the specific internal structure of a GMC and how does this structure affect the mode of star formation in the cloud? What is the relation between clumps, dense cores, and

star formation? Studying the internal structure of GMCs automatically leads to the Orion molecular cloud complex because it is the giant star-forming complex nearest to the Sun. Its two major GMCs L 1641 (Orion A) and L 1630 (Orion B) were the subject of many studies. The first systematic surveys for dense cores (LBS in Orion B, and Tatematsu et al. 1993 in Orion A) and for protostellar condensations in GMCs (Launhardt et al. 1996 in Orion B, and Chini et al. 1997 in Orion A) were performed towards this region. In this chapter, we discuss the distribution of dense gas and dust and the relation of the dense substructures to star formation in the Orion B GMC.

2. General Cloud Properties

The Orion B Molecular Cloud (L 1630) is the northern one of the two major GMCs in the Orion complex (see Chapter of Bally & Heiles). It extends over 40×60 pc ($6^\circ \times 8^\circ$) northward from the Orion Nebula and contains several well-known star-forming regions such as NGC 2071, NGC 2068, M 78 (HH 19–27), NGC 2024, and NGC 2023 (see Fig. 1). The two Orion clouds are located between 320 and 500 pc in distance (Brown et al. 1994). We will use here an average distance of 400 pc, resulting from a study of the distances to B-type stars in the Orion association (Anthony-Twarog 1982). Earlier reviews about the Orion complex can be found in Goudis (1982), Maddalena et al. (1986), Genzel & Stutzki (1989), and Lada et al. (1993).

The large-scale gas distribution of the Orion region has been mapped in ^{12}CO by Kutner et al. (1977) and Maddalena et al. (1986), and in ^{13}CO by Bally et al. (1991). The Orion A and B clouds seem to be physically connected as indicated by the same distances and the presence of a low-level CO emission bridge without a discontinuity in velocity. However, in contrast to the Orion A cloud, the Orion B cloud has no overall velocity gradient. Maddalena et al. (1986) derive a total mass of $8 \times 10^4 M_\odot$ for the Orion B GMC. The CO maps reveal that the gas is not distributed uniformly throughout the cloud. There is a ridge of emission at the western edge of the cloud which contains the two major clumps, connected by lower level CO emission (cf. Figs. 1 and 2). Just to the west of the cloud, the Ia and Ib subgroups of the Orion OBI association are located (see Goudis 1982 for a review). Their strong UV radiation field and stellar winds impinge on the “surface” of the molecular cloud from this side.

The main internal heating source of L 1630 is the H II region NGC 2024 which is the second most luminous source in the Orion region and the only region in the Orion B cloud containing O stars. Further up to the north, the two reflection nebulae NGC 2068 and NGC 2071, which are both associated with compact H II regions, are the dominating internal heating sources.

The Orion B cloud appears to be clumpy on different size scales with the five star-forming regions mentioned above being concentrated in the two major CO clumps which are, again, part of the western ridge (see Fig. 1). These two major clumps are also present in the $100 \mu\text{m}$ dust continuum emission (Fig. 2), which follows in general the CO emission (see Bally et al. 1991 for a discussion of the relation between dust and CO emission). At higher spatial resolution, this structure breaks up into several subclumps, such as NGC 2071 main and NGC 2071 IR (see Fig. 3).

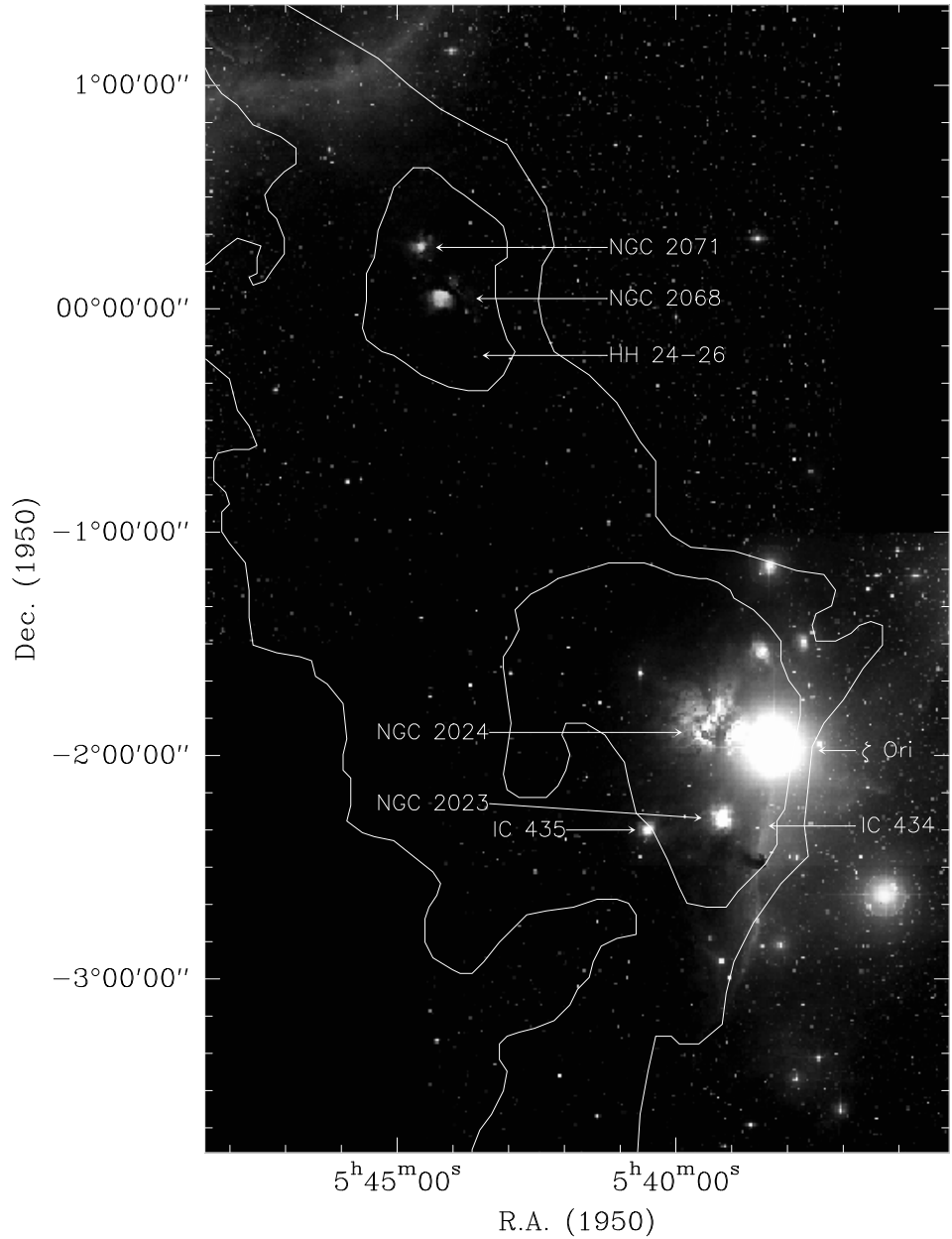


Figure 1. Optical image of the Orion B (L 1630) GMC region, taken from the Digitized Sky Survey. The overlaid contours outline the central part of the molecular cloud. The contours mark the 6.4 and 29 K km s⁻¹ levels of the integrated ¹²CO emission (Maddalena et al. 1986).

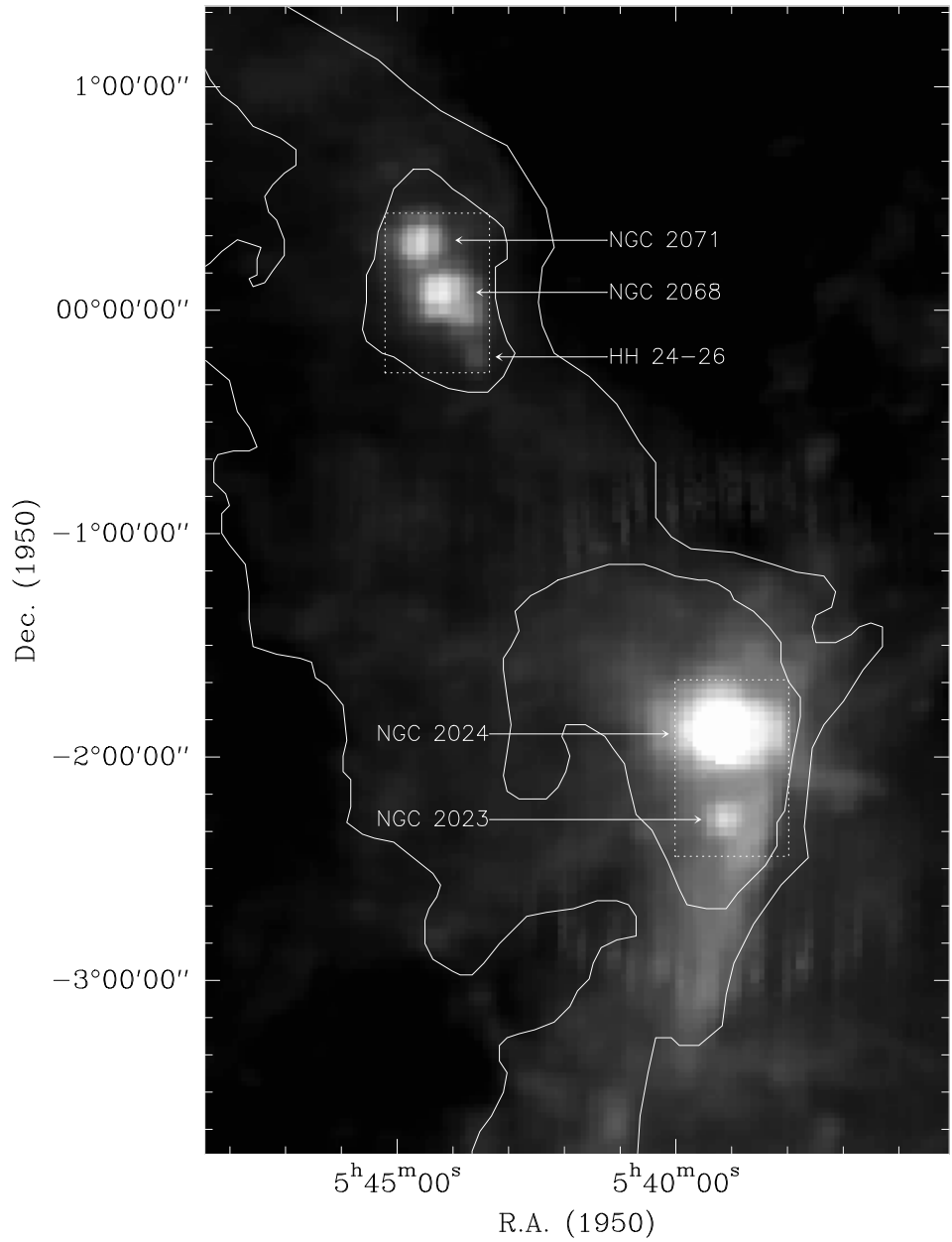


Figure 2. 100 μm IRAS (HiRes) image of the Orion B GMC region. The overlaid contours show the CO cloud (same contours as in Fig. 1). The dotted boxes mark the fields which are enlarged in Fig. 3.

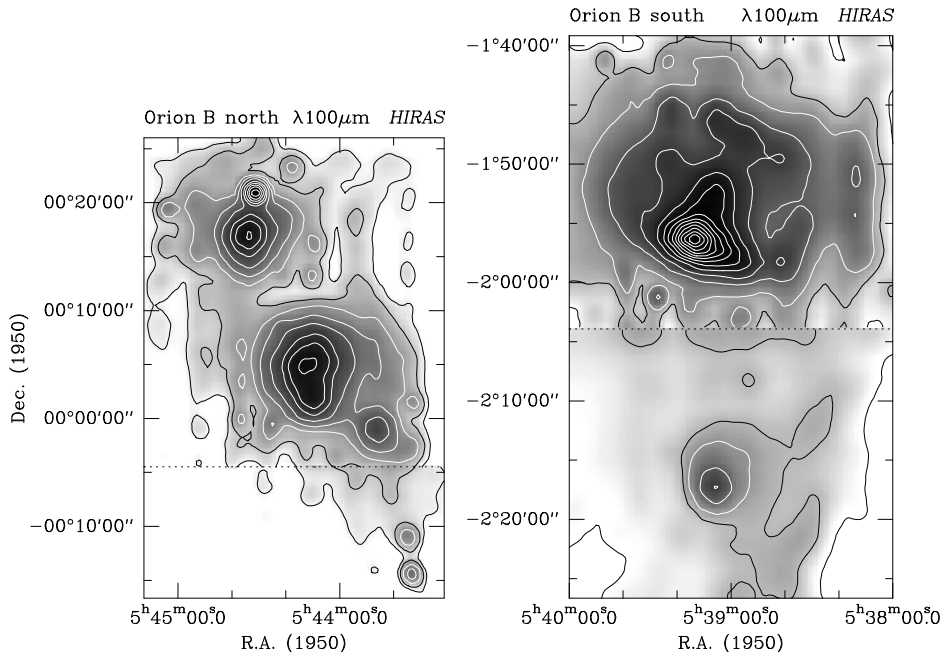


Figure 3. $\lambda 100 \mu\text{m}$ (continuum) *HIRAS* maps of the two major clumps of the Orion B GMC (Launhardt et al. 1996).

3. Dense Cores in the Orion B Molecular Cloud

To investigate the structure and location of the dense gas, the Orion B molecular cloud (L 1630) was systematically surveyed in the $J = 2 \rightarrow 1$ transition of CS (Lada et al. 1991a). The total area covered by the survey was ~ 3.6 square degrees or 20% of the molecular cloud as measured in CO (Maddalena et al. 1986). The beam size (FWHM) of the CS survey was $\sim 1.8'$ which corresponds to 0.21 pc at the distance of Orion. Emission was detected, at a 3σ level above the noise (~ 0.2 K), over $\sim 10\%$ of the area surveyed. The large-scale pattern of the CS emission was found to be similar to that of the CO emission. The majority of the CS emission is concentrated in the two major CO clumps located in the western ridge of the cloud. The CS emission, however, shows much more structure than the CO emission. The survey revealed that the dense CS gas in the Orion B cloud is distributed in a very clumpy manner. Bright CS emission was found in all previously known star-forming regions (see Sect. 2.). In addition to these well-known sources, many previously unknown dense cores were found.

Analyzing the CS data in the position-position-velocity space, 42 separate CS cores were identified at a 5σ level above the noise. The spatial distribution of these cores is shown in Fig. 4. Most of the cores appear to be distributed around a line extending southwest to northeast, following the western ridge of strong CO emission (Maddalena et al. 1986). The CS cores along this ridge are organized into two large clusterings which correspond to the two major CO clumps of the cloud. In addition, these two clusterings, in turn, appear to be organized into subclusters around four of the five most massive cores. The comparison of the

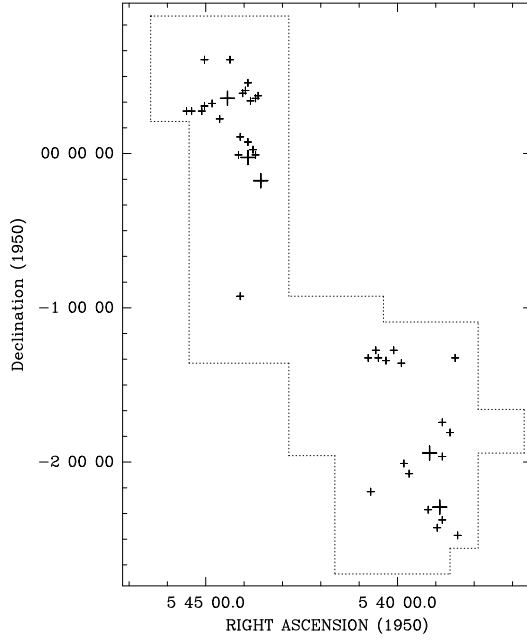


Figure 4. Spatial distribution of the (5σ) CS cores in the Orion B cloud (Figure from Lada et al. 1991a). Plus signs correspond to the positions of peak intensity for each core. Large plus signs represent the five most massive cores identified by the CS survey.

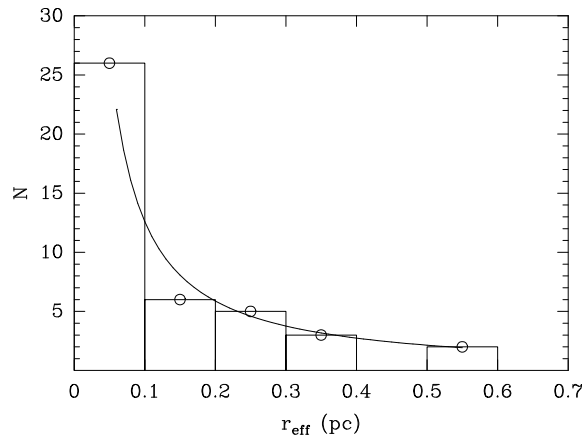


Figure 5. Frequency distribution of core radii (Figure from Lada et al. 1991a). The number of 5σ cores vs. effective radii is plotted as a histogram with bin sizes equal to the beam radius of the survey. The distribution is fitted by the power law: $dN/dr \propto r^{-1.1}$.

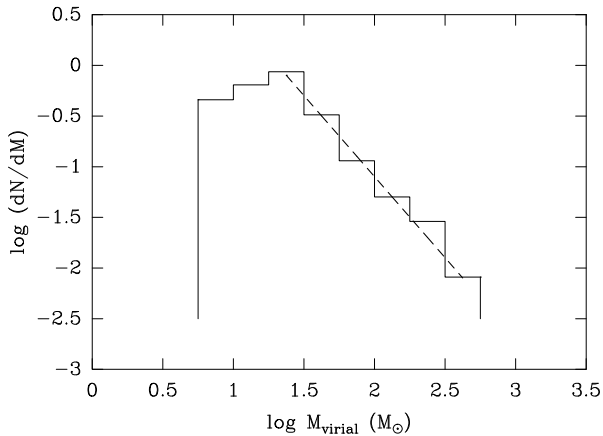


Figure 6. The mass spectrum for dense CS cores in the Orion B cloud (Figure from Lada et al. 1991a). For $M > 20 M_{\odot}$, the mass spectrum is fitted by the power law: $dN/dM \propto M^{-1.6}$. The turnover in the mass spectrum may be due to incomplete sampling.

distribution of the dense gas with the distribution of near-infrared sources (Lada et al. 1991b; see also Chapter of Meyer & Lada) reveals that star formation in the Orion B cloud is highly localized and occurs almost exclusively in the dense gas (Lada 1992). The physical properties of the dense cores as derived from the CS(2–1) emission exhibit a range of properties which are summarized as follows:

1. Core sizes (effective diameter) range from < 0.2 pc (beam size) to 1 pc. The size distribution dN/dr follows a power law with an exponent of -1.1 , indicating that there exist much more small clumps than large ones.
2. Core shapes are not round but appear elongated. The average aspect ratios range from 1.0 to 3.3, with a mean value of 1.8.
3. Core velocity dispersions, σ_v , lie between 0.31 and 0.95 km s^{-1} , with a mean value of 0.58 km s^{-1} . The average core-to-core velocity dispersion is 0.65 km s^{-1} .
4. The virial masses of the individual cores range from < 8 to $500 M_{\odot}$. The mass spectrum of the cores dN/dM is fitted by a power law with an index of -1.6 , indicating that a significant fraction of the mass is located in the most massive cores. Indeed $\sim 50\%$ of the total core mass is contained within the five most massive cores, having masses $> 200 M_{\odot}$. These five cores correspond to the only previously known regions of active star formation in the Orion B cloud (LBS 8 - NGC 2071, LBS 17 - NGC 2068, LBS 23 - HH 24–26, LBS 33 - NGC 2024, and LBS 36 - NGC 2023).
5. The average density of the CS cores is of the order of 10^4 cm^{-3} . However, multi-transition CS observations of four massive dense cores and two low-

mass cores showed that small regions with densities higher than 10^5 cm^{-3} seem to exist in all of the massive cores (Lada et al 1997).

Gibb et al. (1995) mapped six of the 42 LBS CS cores in several molecular transitions with angular resolutions of $14''$ to $60''$ (corresponding to $0.03 - 0.1 \text{ pc}$). These observations revealed that especially the more massive CS cores appear rather filamentary and break up into several sub-cores which continue, thus, the clumpy structure of the cloud down to a length scale of a few hundredths of a parsec. The (virial) masses of these sub-cores are in the range of 3 to $30 M_{\odot}$. The same result was obtained by a multitransition CS study (Lada et al. 1997) which leads to the conclusion that the more massive CS cores appear to be more fragmented than the less massive cores. Comparison of the properties of the dense cores with the content of embedded young stars reveal that massive cores with a large fraction of their gas having densities higher than 10^5 cm^{-3} and a high degree of fragmentation are required to form rich clusters. In contrast, less massive cores which also have small amounts of gas with densities exceeding 10^5 cm^{-3} are mostly less fragmented and seem to produce only small numbers of stars (Lada et al. 1997).

4. Search for Pre-stellar and Protostellar Condensations

The dense CS cores are the places where new stars are formed in the GMC, but they are not the progenitors of individual stars. The “real” protostellar condensations are often overlooked in molecular line surveys although they should in principle be seen, e.g., in higher CS transitions. A basic problem of spectral line observations towards cold dense condensations is the fact that most of the easily observable spectral lines get opaque in regions of high column densities. Many molecules (e.g. CS) may also freeze out on the dust grains in these cold condensations at high column densities and volume densities of $n_{\text{H}} > 10^6 \text{ cm}^{-3}$ (see, e.g., Mezger et al. 1992; Blake et al. 1994; Wiesemeyer et al. 1997). The thermal dust emission at submillimetre/millimetre wavelengths, on the other hand, remains optically thin in these regions and, thus, provides an excellent tracer of protostellar cores. In addition, it yields reliable estimates of hydrogen column densities and masses (see, e.g. Launhardt & Henning 1997).

In order to search for pre-protostellar and protostellar condensations, 25 out of the 42 LBS CS cores were surveyed by Launhardt et al. (1996) in the 1.3 mm continuum emission. The total area covered by this survey was $\sim 800 \text{ arcmin}^2$. All CS cores with virial masses of $> 35 M_{\odot}$ were covered and only the least massive ones were not observed. With a spatial resolution of $23''$ (HPBW) and a 3σ detection limit of $2 M_{\odot}/\text{beam}$ (380 mJy), dust continuum sources were found in 11 out of the 25 CS cores surveyed. Most of these dust condensations were previously unknown. Nine out of the 11 dust sources detected were, in addition, mapped with the MPIfR 7-channel bolometer array at the 30-m IRAM telescope (HPBW = $12''$ corresponding to $\sim 0.02 \text{ pc}$ at the distance of Orion; average 3σ detection limit = $27 \text{ mJy}/\text{beam}$). The higher spatial resolution and sensitivity of the latter observations led to the discovery of very dense ($10^6 - 10^8 \text{ cm}^{-3}$) and compact condensations, but tended to miss the extended envelopes which are better seen in the SEST maps. The survey fields are shown in Fig. 7 and the results of this survey are summarized in Table 2.

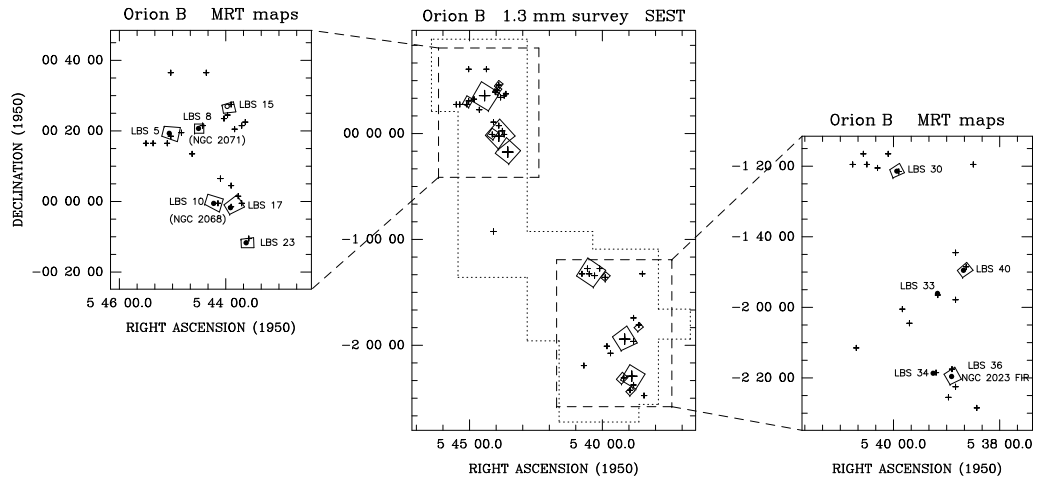


Figure 7. Center: Fields in the Orion B cloud mapped at 1.3 mm continuum with the SEST. Plus signs correspond to the 5σ LBS CS cores. Large plus signs represent the 5 most massive CS cores. The dotted lines mark the boundaries of the CS survey.

Left and right: Fields mapped with the IRAM 30-m telescope at 1.3 mm continuum.

The first remarkable result is that the occurrence of dust condensations appears to be strongly correlated with the virial mass of the CS cores. While nearly all CS cores with $M_{\text{vir}}(\text{CS}) > 100 M_{\odot}$ have embedded dust condensations, nearly none of the less massive CS cores have such condensations (see Fig. 8). The average (virial) mass of the CS cores with dust condensations is $220 M_{\odot}$, while that of the CS cores without dust condensations is only $44 M_{\odot}$. That means that in a GMC large amounts of coherent dense gas is required to initiate local protostellar collapse at all and that the less massive cores are probably unstable. No dust condensations were found really outside of CS cores within the mapped fields. The second result is that the dust condensations are in general much smaller and less massive than the CS cores. This is not surprising because both tracers (CS(2–1) and mm dust continuum) and the corresponding observing methods are sensitive to different physical regimes.

No genuine point sources were detected in the dust continuum emission. Out of the 11 sources detected, four sources are extended and structureless (LBS 5, LBS 15, LBS 34 = NGC 2023, and LBS 40), while seven sources have compact (partially unresolved) condensations surrounded by more or less extended envelopes. These extended dust envelopes correspond to the central, denser parts of the CS cores. If the compact condensations are the true protostars, then such protostars (in GMCs) seem to be always embedded in dense envelopes (CS cores) which are much more massive than they are. The total sizes of the detected dust sources range from 0.02 to 0.5 pc and their masses range from 2 to $200 M_{\odot}$. More interesting are, however, the occurrence and the properties of the compact dust condensations. Such compact condensations were found in the five most massive LBS cores ($M_{\text{vir}} > 200 M_{\odot}$; LBS 8 = NGC 2071, LBS 17 = NGC 2068, LBS 23

= HH 24–26, LBS 33 = NGC 2024, and LBS 36 near NGC 2023) as well as in two LBS cores with $M_{\text{vir}}(\text{CS2-1}) \sim 100 M_{\odot}$ (LBS 10 = NGC 2068, and LBS 30). Their masses range from 1 to $20 M_{\odot}$, and the average hydrogen number densities are of the order of $n(\text{H}_2) \sim 10^6 - 10^8 \text{ cm}^{-3}$. Their sizes (FWHM) range from 0.01 to 0.04 pc (2000–7000 AU). Since the size of these compact condensations corresponds roughly to the “infall radius” $\sim 10^5$ yrs after the start of the protostellar collapse (assuming “inside-out” collapse and an effective sound speed of 0.2 km/s, e.g. Shu 1977), we really see the material which is involved in currently building up new stars. That also means that the masses of the compact dust condensations should be of the order of the masses of the stars they are forming. Consequently, we can conclude that apart from NGC 2024 (LBS 33) and NGC 2071 (LBS 8), no other cores in the Orion B GMC contain enough concentrated mass to be involved in present-day high-mass star formation.

Table 2. Properties of the condensations derived from dust emission.

Source ^(a)	total size ^(b) ($D_{\text{maj}} \times D_{\text{min}}$) (pc ²)	core size ^(c) ($D_{\text{maj}} \times D_{\text{min}}$) (pc ²)	$M_{\text{g}}^{\text{tot}(d)}$ (M_{\odot})	$M_{\text{g}}^{\text{core}(d)}$ (M_{\odot})	$n(\text{H}_2)^{\text{core}(e)}$ (cm^{-3})	Associated IR source
LBS 5 SM	0.06×0.02	–	2.4	–	–	IPSC, NIR
LBS 8 SM	0.15×0.14	0.025×0.017	50	10	3.2×10^7	IPSC, NIR ^(f)
LBS 10 SM	0.05×0.05	0.035×0.027	4.4	2.3	2.3×10^6	IPSC, NIR
LBS 15 SM	0.09×0.06	–	4.4	–	–	–
LBS 17 SM	0.06×0.04	0.017×<0.012	4.0	1.7	$>1.7 \times 10^7$	–
LBS 23 SM ^(g)	0.07×0.04	0.023×<0.012	30	4.0	$>2.5 \times 10^7$	NIR ^(h)
LBS 30 SM	0.12×0.07	0.014×<0.012	3.8	1.0	$>1.3 \times 10^7$	IPSC
LBS 33 SM ⁽ⁱ⁾	0.46×0.35	...	500 ^(j)	4–20 ^(j)	$9-50 \times 10^7$ ⁽ⁱ⁾	NIR ^(k)
LBS 34 SM	0.33×0.23	–	100	–	–	–
LBS 36 SM1	0.14×0.11 ^(l)	0.014×<0.012	24 ^(l)	5.6	$>7.4 \times 10^7$	–
LBS 36 SM2	...	0.025×0.019	...	1.5	4.1×10^6	–
LBS 40 SM	0.23×0.14	–	23	–	–	–

^(a)SM refers to the submillimetre source detected in the CS core;

^(b)FWHM, depends on map size and sensitivity;

^(c)FWHM, deconvolved with beam size. Refers to the central, compact dust condensations;

^(d)Total gas mass, including helium and metals;

^(e) H_2 volume density, core mass divided by volume;

^(f)Rich embedded cluster. The strongest source is NGC 2071 IRS 1 (Aspin et al. 1992) at the mm peak position;

^(g)HH 24 SMM, Chini et al. 1993;

^(h) H_2 jet discovered by Bontemps et al. 1996

⁽ⁱ⁾NGC 2024, Mezger et al. 1988 and 1992: seven compact dust condensations (FIR 1–7) embedded in a common envelope;

^(k)See Chapter by Meyer & Lada;

^(l)Two condensations were found in LBS 36. These numbers refer to the common envelope;

In combination with near-, mid- (Launhardt et al. 1997), and far-infrared data, the dust continuum maps also provide information about the evolutionary stage of the condensations (see Table 3). If the dust source is extended with-

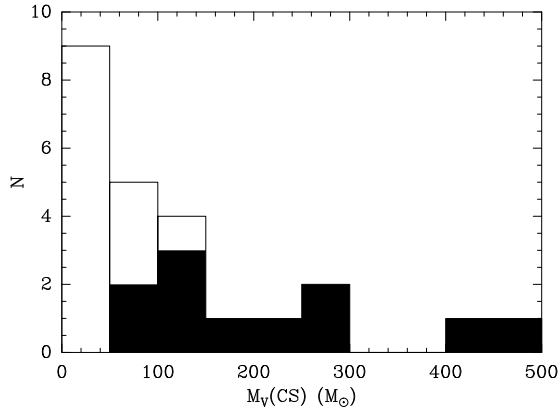


Figure 8. Frequency distribution of core masses of the CS cores observed at $\lambda 1.3$ mm. The number of cores is plotted vs. their virial mass derived from CS(2–1) (Lada et al. 1991a). Black bars correspond to the CS cores in which dust condensations were detected. Bin sizes correspond to $50 M_{\odot}$.

out any compact condensation and is also not associated with near-IR sources, it is probably unstable or in a pre-protostellar phase (Ward-Thompson et al. 1994). Observed extents of ~ 0.1 pc and average hydrogen densities of the order of 10^6 cm^{-3} favour the pre-protostellar phase for LBS 15 SM and LBS 40 SM. The very extended filament LBS 34 SM may contain or form such cores, but they were not resolved.

The small extents (< 0.02 pc) and the high average densities ($\sim 10^7 \text{ cm}^{-3}$) of the dust condensations in LBS 17 and LBS 36 imply that they are more evolved. The lack of any detectable infrared emission up to $100 \mu\text{m}$, on the other hand, implies that these condensations cannot yet harbour strong heating sources as, e.g., young stars. They are, therefore, good candidates for being protostellar objects in their earliest phase of formation, although direct observational evidence of star formation activity (e.g. mass infall) is still lacking. The discovery of seven compact dust condensations by Mezger et al. (1988, 1992) in the NGC 2024 cloud core (LBS 33) has stimulated many controversial discussions about the true nature of these objects. For several of these condensations there exists now evidence that they contain embedded protostars at a very early stage or young stars (e.g. Chandler & Carlstrom 1996, Wiesemeyer et al. 1997, and references therein; see also Chapter by Meyer & Lada). Another very young protostellar condensation is LBS 23 SM (HH 24 SMM, discovered by Chini et al. (1993) which was recently confirmed to be a “Class 0” protostar (e.g. Krügel & Chini 1994, Ward-Thompson et al. 1995, Bontemps et al. 1995, 1996).

More evolved, but still very compact dust condensations are LBS 8 SM, LBS 10 SM, and LBS 30 SM which all contain infrared sources. LBS 8 SM is identical with the region of active star formation NGC 2071 IR which is located $4'$ north of the reflection nebula NGC 2071. It is associated with a rich near-

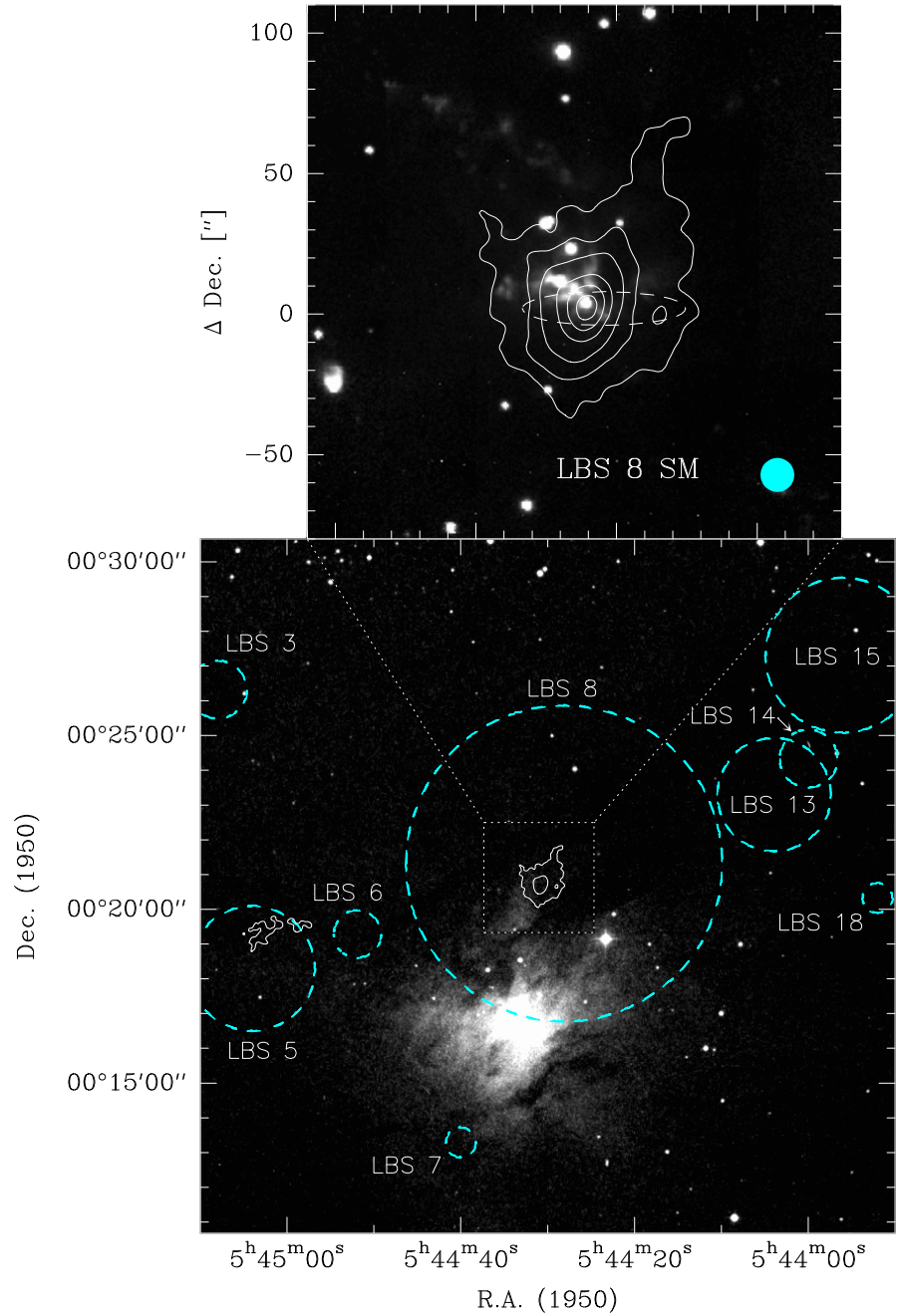


Figure 9. Optical image of the NGC 2071 region taken from the Digitized Sky Survey (lower box). The dashed circles represent the LBS CS cores (mean diameters). The solid contours show the 1.3 mm dust condensation. The enlarged field (upper box) is an overlay of a deep NIR K-band image and the 1.3 mm continuum contours (100 to 2000 mJy/beam). The dashed ellipse marks the IRAS point source (position error ellipse). The filled grey circle represents the 1.3 mm beam.

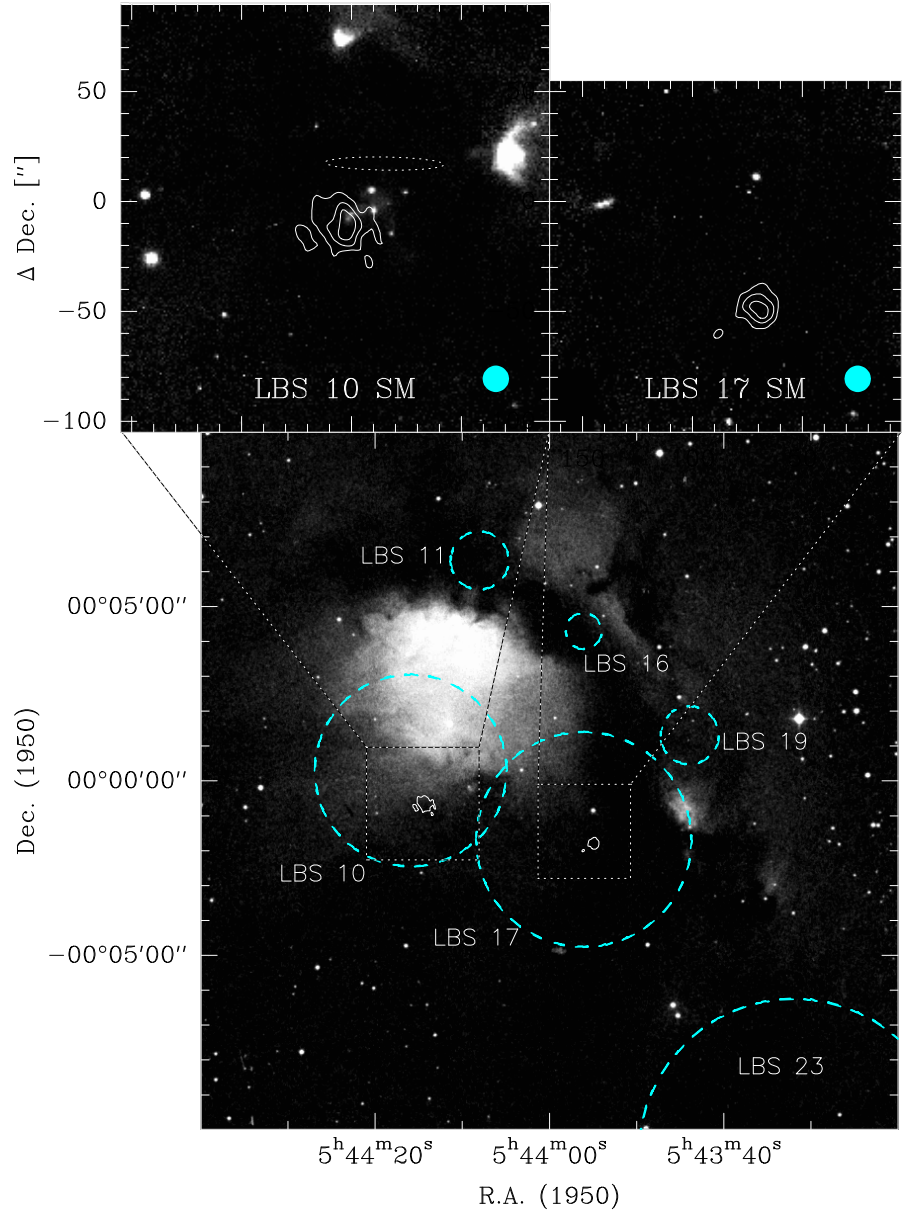


Figure 10. Optical image of the NGC 2068 region taken from the Digitized Sky Survey (lower box). The dashed circles represent the LBS CS cores (mean diameters). The solid contours show the 1.3 mm dust condensations. The enlarged fields (upper boxes) are overlays of deep NIR K-band image and the 1.3 mm continuum contours (100 to 300 mJy/beam). The dashed ellipse marks the IRAS point source (position error ellipse). The filled grey circles represent the 1.3 mm beam.

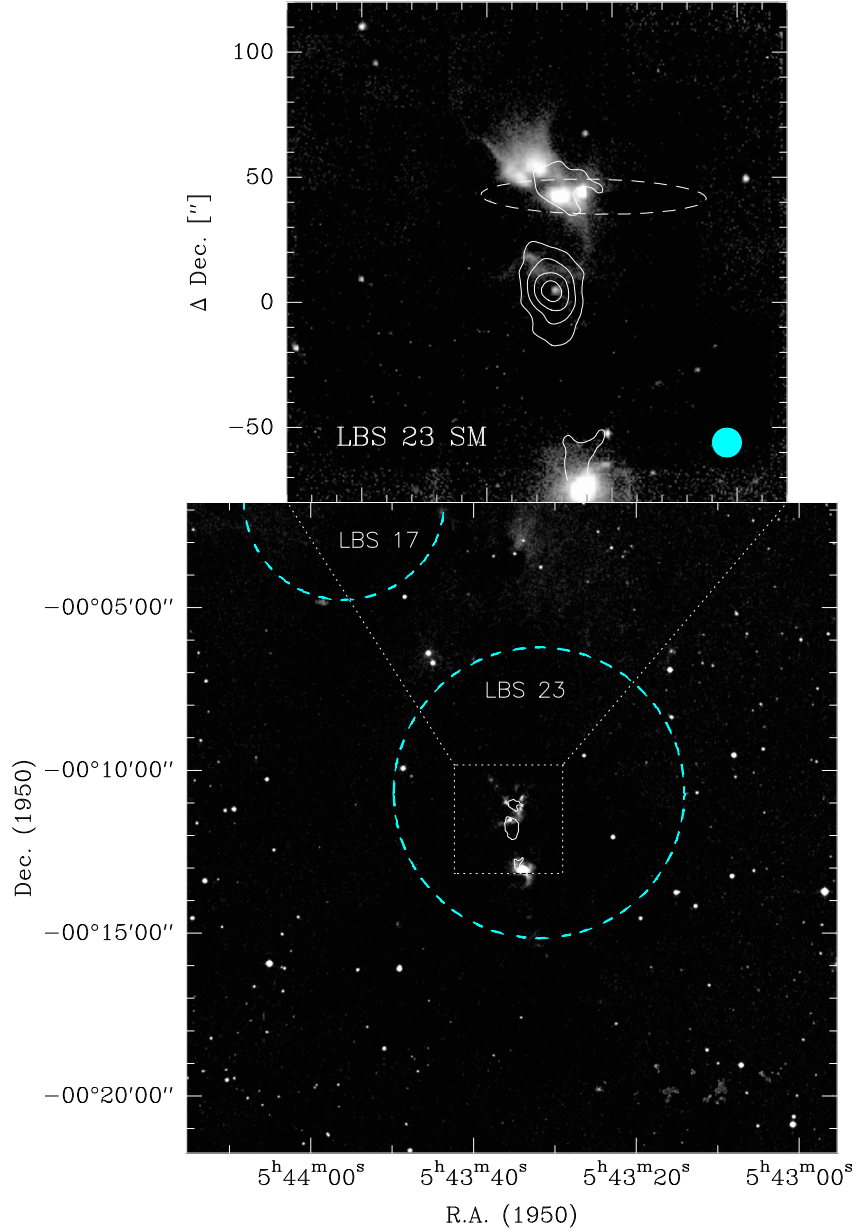


Figure 11. Optical image of the HH 24–26 region taken from the Digitized Sky Survey (lower box). The dashed circles represent the LBS CS cores (mean diameters). The solid contours show the 1.3 mm dust condensations. The enlarged field (upper box) is an overlay of a deep NIR K-band image and the 1.3 mm continuum contours (120 to 1000 mJy/beam). The dashed ellipse marks the IRAS point source (position error ellipse). The filled grey circle represents the 1.3 mm beam.

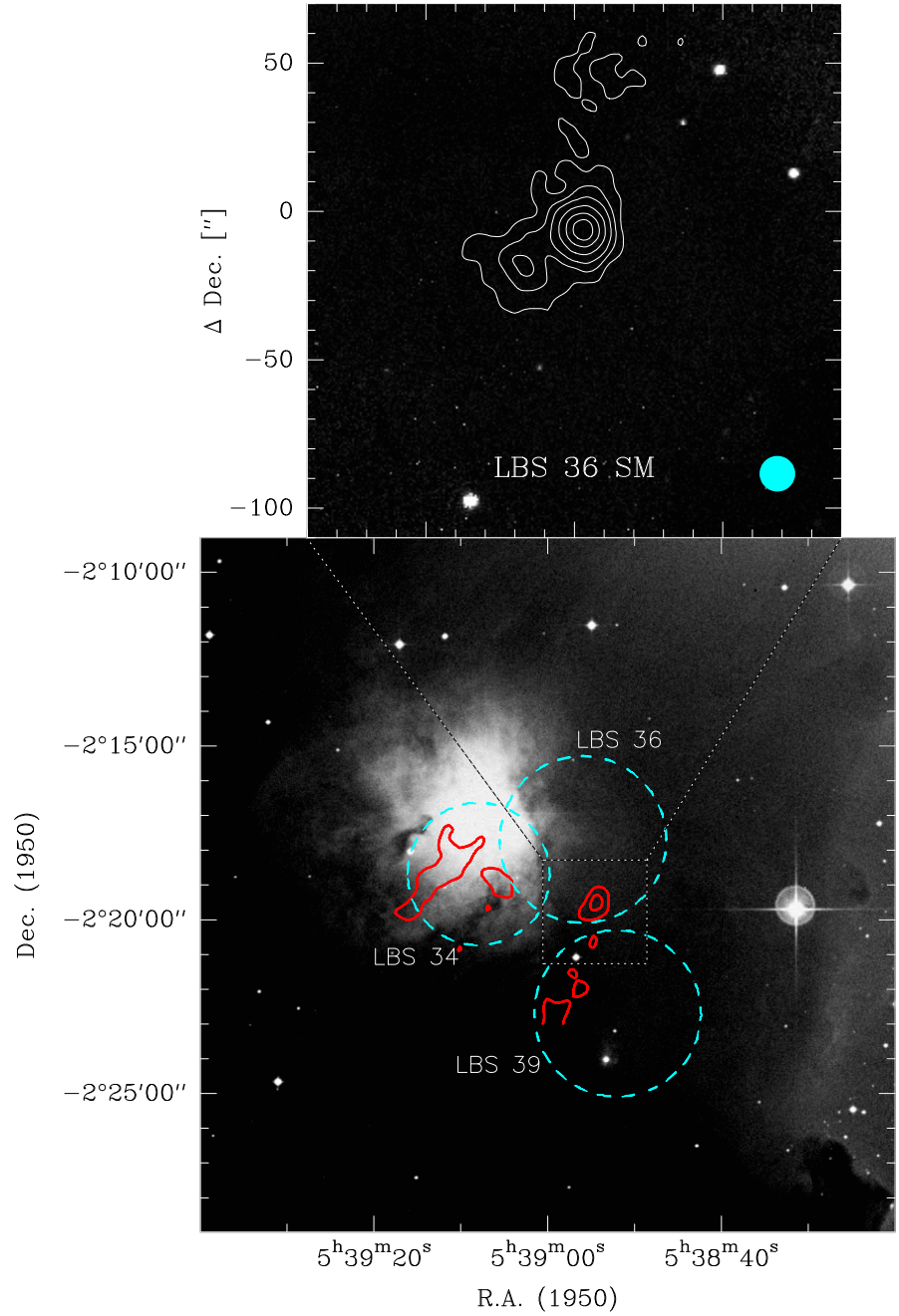


Figure 12. Optical image of the NGC 2023 region taken from the Digitized Sky Survey (lower box). The dashed circles represent the LBS CS cores (mean diameters). The solid contours show the 1.3 mm dust condensations. In the lower right corner, the Horsehead Nebula is seen. The enlarged field (upper box) is an overlay of a deep NIR K-band image and the 1.3 mm continuum contours (75 to 1200 mJy/beam). The filled grey circle represents the 1.3 mm beam.

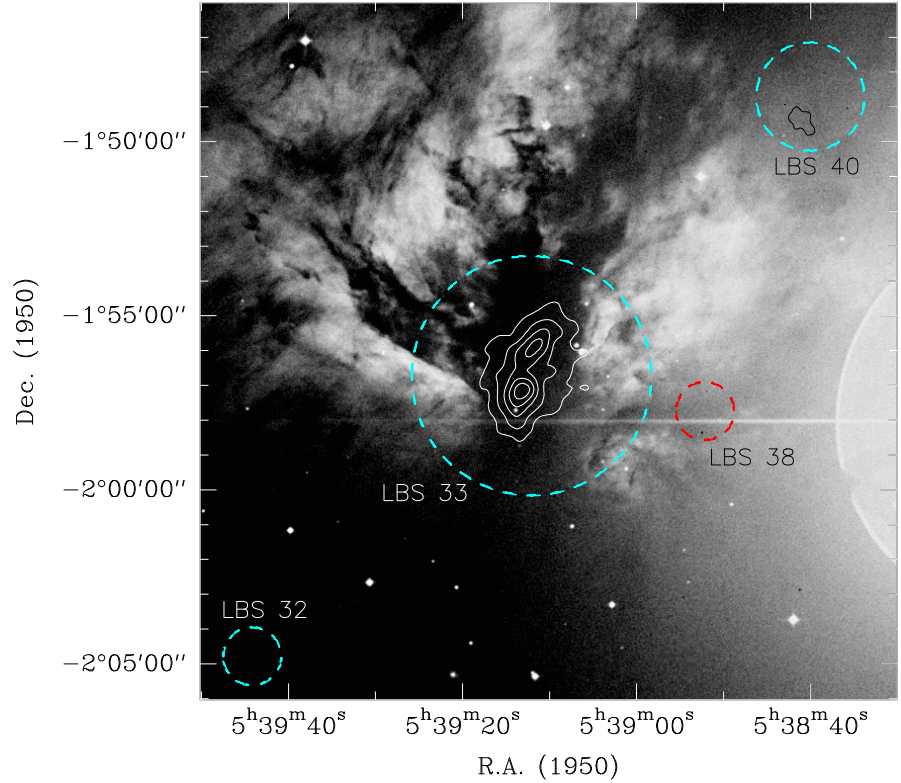


Figure 13. Optical image of the NGC 2024 region taken from the Digitized Sky Survey. The dashed circles represent the LBS CS cores (mean diameters). The solid contours show the 1.3 mm dust condensations.

Table 3. Morphology of the dust condensations and association with infrared sources.

	extended dust emission no compact condensation	compact condensation (with envelope)
No IR source	LBS 15 SM, LBS 34 SM LBS 40 SM	LBS 17 SM, LBS 36 SM 1/2 LBS 33 FIR 1–7 ^a
NIR or IRAS source	LBS 5 SM	LBS 8 SM, LBS 10 SM LBS 23 SM ^b , LBS 30 SM

^aThe NGC 2024 core has seven protostellar condensations embedded in a common envelope, being in different evolutionary stages. Mezger et al. 1988 and 1992; Chandler & Carlstrom 1996; Wiesemeyer et al. 1997; FIR 4 is associated with a $2\mu\text{m}$ source - Moore & Chandler 1989.

^bLBS 23 SM = HH 24 SMM (Chini et al. 1993) is associated with a near-IR (H_2) jet emanating from the protostellar core (Bontemps et al. 1996)

infrared cluster (Persson et al. 1981; Walther et al. 1991, 1993), with a high-velocity bipolar outflow (e.g., Bally 1982; Snell et al. 1984). The major part of the dust emission clearly originates from a very compact condensation which coincides in position with the near-IR source IRS 1. The presence of several H₂O masers (e.g. Genzel & Downes 1979), of an OH maser (Johansson et al. 1974), as well as of compact HII regions (Gilmore 1980) indicate that active high-mass star formation is going on in this region (see also Aspin et al 1992).

The diffuse dust source LBS 5 SM is associated with a near-IR nebula and a 10 μ m source (Launhardt et al. 1997). The dust continuum emission of this source is, therefore, assumed to originate from the remnant of the former protostellar core. LBS 5 SM is so far the most evolved dust continuum source detected in this survey.

5. Conclusion

Giant Molecular Clouds are complex creations with the gas and dust organized in a hierarchical structure. Observations of different tracers at different spatial resolutions are required in order to detect the complexity of this structure and to reveal the relationship between the global properties of the GMC on the upper end of the scale and the star formation which takes place inside the cloud on much smaller scales. The cloud as a whole is made of relatively thin gas and large clumps of dense gas being made of subclumps, which in turn are made of smaller and denser subclumps (dense cores). Many, but by far not all of these dense cores contain high-density condensations which are the progenitors of individual stars or bound clusters of stars. Systematic surveys for dense cores, protostellar condensations, and embedded young stars (see Chapter by Meyer & Lada) in the Orion B cloud have revealed the structure of the gas and dust over a size scale ranging from 10 pc down to 0.01 pc and the relation of this structure to the recent and current star formation in the cloud.

The gas is not distributed uniformly throughout the Orion B cloud; rather it is very clumpy. Less than 20% of the total gas mass of the cloud is confined in dense cores ($n \geq 10^4 \text{ cm}^{-3}$). Of this dense gas, 50% is located in the five most massive cores, which in turn are concentrated in the two major clumps of the GMC. The dense cores have typical sizes of 0.1 to 0.5 pc. Their masses range from 10 to 500 M_{\odot} with a mass spectrum of $dN/dM \sim M^{-1.6}$, indicating that a significant mass fraction of the dense gas is located in the most massive cores. Especially the more massive CS cores have a large fraction of their gas with densities exceeding 10^5 cm^{-3} . These cores tend to be more fragmented than the less massive cores and form rich clusters of stars. Protostellar condensations which have much higher densities (10^6 to 10^8 cm^{-3}) were preferentially found within the boundaries of such massive CS cores ($M_{\text{core}} > 100 M_{\odot}$). These protostellar condensations have typical masses and sizes of 1 to 10 M_{\odot} and 0.01 to 0.04 pc, respectively. In contrast, less massive CS cores appear ($M_{\text{core}} > 100 M_{\odot}$) to be mostly less fragmented and contain nearly no detectable protostellar condensations. These cores produce only small numbers of stars but no rich clusters.

All previously known regions of star formation such as NGC 2071, NGC 2068, M 78 (HH 19–27), NGC 2024, and NGC 2023 are associated with massive, dense cloud cores. Protostellar condensations were found in all of these regions, indi-

cating that star formation is still going on there. However, apart from NGC 2024 and NGC 2071, we find no other regions which contain enough concentrated mass to be involved in present-day high-mass star formation. Apart of these two regions, only less massive protostellar condensations which will form low to intermediate-mass stars were found. The lack of clusters of protostars in the other large star-forming regions indicates that they are more evolved and have transformed most of their dense gas into stars. It also suggests that star formation occurs rather episodically than continuously in such massive dense cores. Altogether, it is concluded that the general picture of star formation reflects the distribution of the dense gas: Most stars in the Orion B cloud are formed in the clustered mode with the most active star formation going on in the most massive dense cores. The rich clusters of stars seem to form from very massive and dense cores due to fragmentation rather than due to aggregation of a distributed population of smaller units.

Nearly all of the dense gas and the current star formation is concentrated in a ridge at the western edge of the elongated Orion B cloud where the strong UV radiation and the stellar winds from the Orion OB I association impinge on the cloud “surface”. It is, therefore, natural to assume that the young and massive stars of the OB I association triggered the current star formation within the cloud due to the one-sided compression of the gas. While it can be understood in this context that some (or most) giant molecular clouds form rich clusters of stars, it is less clear why, independent of mass, no distributed star formation takes place in the Orion GMCs as it is observed, e.g., in the Taurus dark clouds. One reason might be that the massive stars formed in the massive cores of GMCs compress, disturb, and mix the gas in the cloud on time scales which are too short to allow isolated, low-mass dense cores to overwhelm the turbulent or magnetic support and to form finally stars.

Acknowledgments. RL acknowledges support through the Verbundforschung Astronomie und Astrophysik, contract No. 50 OR 9414 9.

References

- André, P., Ward-Thompson, D., & Barsony, M. 1993, *ApJ*, 406, 122
Anthony-Twarog, B.J. 1982, *AJ*, 87, 1213
Aspin, C., Sandell, G., & Walther, D.M. 1992, *MNRAS*, 258, 684
Bally, J. 1982, *ApJ*, 261, 558
Bally, J., Langer, W.D., & Liu, W. 1991, *ApJ*, 383, 645
Benson, P.J. & Myers, P.C. 1989, *ApJS*, 71, 89
Blake, G.A., van Dishoeck, E.F., Jansen, D.J., Groesbeck, T.D., & Mundy, L.G. 1994, *ApJ*, 428, 680
Blitz, L. 1993, in *Protostars and Planets III*, Levy, E.H. & Lunine, J.I., Tucson: Univ. Arizona Press, 125
Blitz, L., Shu, F.H. 1980, *ApJ*, 238, 148
Blitz, L. & Williams, J.P. 1997, *ApJ*, in press
Bontemps, S., André, P., & Ward-Thompson, D. 1995, *A&A*, 297, 98

- Bontemps, S., Ward-Thompson, D., & André, P. 1996, *A&A*, 314, 477
- Brown, A.G.A., de Geus, E.J., & de Zeeuw, P.T. 1994, *A&A*, 289, 101
- Chandler, C.J., Gear, W.K., Sandell, G., Hayashi, S., Duncan, W.D., & Griffin, M.J. 1990, *MNRAS*, 243, 330
- Chandler, C.J. & Carlstrom, J.E. 1966, *ApJ*, 466, 338
- Chini, R., Krügel, E., Haslam, C.G.T., Kreysa, E., Lemke, R., Reipurth, B., Sievers, A., & Ward-Thompson, D. 1993, *A&A*, 272, L5
- Chini, R., Reipurth, B., Ward-Thompson, D., Bally, J., Nyman, L.-A., Sievers, A., & Billawala, Y. 1997, *ApJ*, 474, L135
- Elmegreen, B.G. & Falgarone, E. 1996, *ApJ*, 471, 816
- Falgarone, E., Phillips, T.G., & Walker, C.K. 1991, *ApJ*, 378, 186
- Genzel, R. & Downes, D. 1979, *A&A*, 72, 234
- Genzel, R. & Stutzki, J. 1989, *ARA&A*, 27, 41
- Gibb, A.G., Little, L.T., Heaton, B.D., & Lehtinen, K.K. 1995, *MNRAS*, 277, 341
- Gilmore, W. 1980, *AJ*, 85, 894
- Goldsmith, P.F. 1987, in *Interstellar Processes*, Hollenbach, D.J. & Thronson Jr., H.A., Dordrecht: Reidel, *Ap&SS Library*, 134, 51
- Goudis, C. 1982, *The Orion Complex: A Case Study of Interstellar Matter*, Dordrecht: Reidel, *Ap&SS Library*, Vol. 90
- Harju, J., Walmsley, C.M., & Wouterloot, J.G.A. 1991, *A&A*, 245, 643
- Johansson, L.E.B., Höglund, B., Winnberg, A., Nguyen-Q-Rieu, & Goss, W.M. 1974, *ApJ*, 189, 455
- Krügel, E. & Chini, R. 1994, *A&A*, 287, 947
- Kutner, M.L., Tucker, K.D., Chin, G., & Thaddeus, P. 1977, *ApJ*, 215, 521
- Lada, E.A. 1992, *ApJ*, 393, L25
- Lada, E.A., Bally, J. & Stark A.A. 1991a, *ApJ*, 368, 432 (LBS)
- Lada, E.A., DePoy, D., Evans, N.J. II, & Gatley, I. 1991b, *ApJ*, 371, 171
- Lada, E.A., Strom, K.M., & Myers, P.C. 1993, in *Protostars and Planets III*, Levy, E.H. & Lunine, J.I., Tucson: Univ. Arizona Press, 245
- Lada, E.A., Evans, N.J. II, & Falgarone, E. 1997, *ApJ*, in press
- Launhardt, R., Mezger, P.G., Haslam, C.G.T., Kreysa, E., Lemke, R., Sievers, A., & Zylka, R. 1996, *A&A*, 312, 569
- Launhardt, R. & Henning, Th. 1997, *A&A*, in press
- Launhardt, R., Käufl, H.U., Stanke, T., & Zinnecker, H. 1997, in preparation
- Linke, R.A. & Goldsmith P.F. 1980, *ApJ*, 235, 437
- Maddalena, R.J., Morris, M., Moscowitz, J., & Thaddeus, P. 1986, *ApJ*, 303, 375
- Mezger, P.G. 1994, *ApSS*, 212, 197
- Mezger, P.G., Chini, R., Kreysa, E., Wink, J., & Salter, C.J. 1988, *A&A*, 191, 44
- Mezger, P.G., Sievers, A.G., Haslam, C.G.T., Kreysa, E., Lemke, R., Mauersberger, R. & Wilson, T.L. 1992, *A&A*, 256, 631

- Moore, T.J.T. & Chandler, C.J. 1989, MNRAS, 241, 19P
- Myers, P.C. & Benson, P.J. 1983, ApJ, 266, 309
- Persson, S.E., Geballe, T.R., Simon, T., Lonsdale, C., & Baas, F. 1981, ApJ, 251, L85
- Plume, R., Jaffe, D.T., Evans, N.J. II, Martin-Pintado, J., & Gomez-Gonzales, J. 1997, ApJ, 476, 730
- Shu, F.H. 1977, ApJ, 214, 488
- Shu, F.H., Adams, F.C., & Lizano, S. 1987, ARA&A, 25, 23
- Snell, R.L., Scoville, N., Sanders, D.B., & Erickson, N.R. 1984, ApJ, 284, 176
- Tatematsu, K., Umenoto, T., Kameya, O., Hirano, N., Hasegawa, T., et al. 1993, ApJ, 404, 643
- Walther, D.M., Geballe, T.R., & Robson, E.I. 1991, ApJ, 377, 246
- Walther, D.M., Robson, E.I., Aspin, C., & Dent, W.R.F. 1993, ApJ, 418, 310
- Ward-Thompson, D., Scott, P.F., Hills, R.E., & André, P. 1994, MNRAS, 268, 276
- Ward-Thompson, D., Chini, R., & Krügel, E. 1995, MNRAS, 274, 1219
- Wiesemeyer, H., Guesten, R., Wink, J.E., & Yorke, H.W. 1997, A&A, 320, 287
- Wouterloot, J.G.A., Walmsley, C.M., & Henkel, C. 1988, A&A, 203, 376
- Zinnecker, H. 1990, in Physical Processes in Fragmentation and Star Formation, Capuzzo-Dolcetta, R., Chiosi, C., & Di Fazio, A., Dordrecht: Kluwer, 201